J Biol Inorg Chem (2009) 14:643–651
DOI 10.1007/s00775-009-0511-y

MINIREVIEW

Recent developments of the quantum chemical cluster approach for modeling enzyme reactions

Per E. M. Siegbahn · Fahmi Himo

Received: 23 January 2009 / Accepted: 28 April 2009 / Published online: 13 May 2009

Abstract The quantum chemical cluster approach for modeling enzyme reactions is reviewed. Recent applications have used cluster models much larger than before which have given new modeling insights. One important and rather surprising feature is the fast convergence with cluster size of the energetics of the reactions. Even for reactions with significant charge separation it has in some cases been possible to obtain full convergence in the sense that dielectric cavity effects from outside the cluster do not contribute to any significant extent. Direct comparisons between quantum mechanics (QM)-only and QM/molecular mechanics (MM) calculations for quite large clusters in a case where the results differ significantly have shown that care has to be taken when using the QM/MM approach where there is strong charge polarization. Insights from the methods used, generally hybrid density functional methods, have also led to possibilities to give reasonable error limits for the results. Examples are finally given from the most extensive study using the cluster model, the one of oxygen formation at the oxygen-evolving complex in photosystem II.

Keywords Computational chemistry · Density functional theory · Molecularmodeling · Photosynthesis

P. E. M. Siegbahn (✉)
Department of Physics,
ALBA NOVA,
Arrhenius Laboratory,
Stockholm University,
106 91 Stockholm, Sweden
e-mail: ps@physto.se

P. E. M. Siegbahn
Department of Biochemistry and Biophysics,
Arrhenius Laboratory,
Stockholm University,
106 91 Stockholm, Sweden

F. Himo
Department of Theoretical Chemistry,
School of Biotechnology,
Royal Institute of Technology,
106 91 Stockholm, Sweden

Introduction

In the cluster approach for modeling enzyme reactions, a limited number of atoms are taken out of the enzyme to represent the active site. All atoms in the model are then treated quantum mechanically at the highest possible level, which so far has mainly meant hybrid density functional theory (DFT). To adapt to the enzyme surrounding, atoms in the periphery of the model are held fixed from available X-ray structures, and the model is placed in a dielectric cavity to give polarization effects. For enzymes containing transition metals, this model has been in use for a little more than a decade [1]. In the beginning, the models contained 20–30 atoms and the geometries were optimized without enzyme constraints. At present, models with up to 200 atoms are often used, which should yield higher accuracy but has also introduced several new problems in the modeling, for example, a large number of local geometric minima. These problems are minimized by trying to limit the model to include only those residues that are found to give significant effects. When this is successful, the approach is extremely powerful and has yielded a wealth of new information. The recent development of this type of modeling is described in the present review.

In contrast, the quantum mechanics (QM)/molecular mechanics (MM) method[1] [2] tries to describe a much

[1] For a recent comprehensive review on QM/MM methods for biological systems see Ref. [2].

larger part of the active site, sometimes even the entire enzyme. A small part around the active site is described quantum mechanically, while the rest of the model is described by classical force fields. The price paid for describing a large fraction of the enzyme is that an extremely large number of local minima are obtained, and procedures to account for this problem are therefore necessary. Clearly, the cluster approach and the QM/MM method can be continuously transformed into each other by increasing the QM part and decreasing the MM part in the QM/MM method. However, the typical difference between the approaches is that the QM part is much larger in the cluster approach, and the MM part is very big in the QM/MM approach.

Methods

The most useful electronic structure method for treating large molecular systems during the past few decades has been the hybrid DFT method with the B3LYP exchange–correlation functional [3]. In spite of numerous attempts, the accuracy of this functional has been difficult to improve upon. The experience using the B3LYP functional for enzyme active sites containing transition metals was reviewed a few years ago [4]. As for other DFT methods, there are three major sources of error. The first one is the self-interaction error, which gives a nonzero contribution for the interaction of an electron with itself. The second error is due to the inherent single determinant description, which, for example, does not allow a proper dissociation of bonds in all cases. This deficiency is sometimes termed "lack of static correlation" or "missing near-degeneracy effects." The lack of static correlation and the self-interaction error cancel to a large extent in most cases. In fact, it can be argued that the functionals are optimized for this cancellation. Therefore, removing one of the errors normally leads to larger total errors. The third error is the lack of van der Waals interaction, which can lead to significant errors when large systems interact, such as for the binding in the chlorophyll dimer in the reaction center of photosynthesis.

A characteristic feature of ab initio methods is that the results can be systematically improved. By extending the basis set and the configuration space, the results will approach the correct result for the model used. This is not possible for DFT and is a significant drawback. Still, one of the most important developments during the past few years is that approaches have been obtained by which one can get a reasonable idea of the accuracy of the results without having to go to a direct comparison with known experimental results. Such comparisons are often not possible owing to a lack of accurate experiments. Instead, it has been realized that the most sensitive parameter in the hybrid DFT method is the amount of exact exchange in the functional. In B3LYP this amount is 20%. For transition-metal-containing systems, it has quite generally been found that using 15% exact exchange instead represents an improvement [5]. Moreover, by variation of the amount of exact exchange, a general empirical rule has been found [6]. The finding is that if the result does not change when the amount of exact exchange is decreased from 20 to 15%, the results are reliable. No exceptions have been found so far. A recent hybrid DFT study on NiFe hydrogenase is illustrative of how this rule can be used in practice [7]. It was found that an end-on peroxide structure was strongly preferred (by more than 10 kcal/mol) compared with the experimentally determined structure with a side-on peroxide. This was found even for models of the active site bigger than 100 atoms. A few years ago, the conclusion would have been that there is something wrong with the hybrid DFT functional. However, when it was found that the result for NiFe hydrogenase was the same whether 20 or 15% exact exchange was used, the conclusion was instead that there is something significant missing in the chemical model, even though it was quite large by normal standards. In later investigations the chemical model was indeed found to be too small, and the B3LYP functional was in fact found to be very accurate for this case. The preferred structure for the larger model is in good agreement with the experimentally determined one.

The first significant improvement of the hybrid DFT method was presented rather recently [8, 9]. In this approach, termed "double hybrid DFT," the errors of DFT mentioned above are directly addressed. The lack of van der Waals effects is corrected by adding an empirical attractive long-range-dispersion correction to the functional. The more difficult problem, the lack of static correlation in DFT, is corrected by also performing a multideterminantal MP2 calculation, and the result of that calculation is weighted with a rather small factor (0.27) into the functional. Since the inclusion of explicit static correlation disturbs the cancellation with the self-interaction error, the amount of exact exchange also has to be substantially increased. This happens automatically in the fitting of the parameters to benchmark tests, and the amount of exact exchange increases from 20% in B3LYP all the way to 53% in the double hybrid method. By these changes, the double hybrid DFT is significantly better than B3LYP for the large general benchmark tests that contain first- and second-row atoms.

The double hybrid DFT method has only recently been tested also for transition-metal-containing systems. In some cases the results are promising [10]. For other systems, such as the notoriously difficult copper dimers with dioxygen, or for ligand binding to heme systems, the results are unfortunately not yet very useful. The problem is the MP2

correction for static correlation, which is often largely overestimated. This problem might be overcome in the future by a reparameterization, which should damp this correction even further from the present factor of 0.27. There is a chance that this could work without severely destroying the good performance for first- and second-row atoms too much, since the total effect of the MP2 correction for these elements is rather small. As a parallel, it has been possible to improve the performance of B3LYP for transition metals by decreasing the amount of exact exchange to 15% without destroying the results for the lighter elements.

On the other hand, removing the MP2 correction, while keeping the explicit correction for van der Waals effects in the double hybrid method, already appears to be quite useful also for transition metals. An example is the binding of CO and NO to heme complexes. A careful analysis using the CASPT2 method has recently demonstrated that B3LYP underestimates the binding in these systems by as much as 10–15 kcal/mol [11]. The dispersion correction computed from the empirical formula is of the order of 10 kcal/mol and therefore improves the results significantly.

Cluster size convergence and long-range polarization

The advances in the DFT methods described in the previous section, coupled with the ever-increasing computer speed, have made it possible to treat also large systems, with quite high accuracy. This has allowed the cluster models of enzyme active sites to become larger and larger. Quite recently, a few systematic studies have appeared investigating the influence of the size of the cluster model on the calculated energies. One issue of particular interest has been the influence of the homogeneous surrounding on the energies and its dependence on the size of the cluster model. Here, we will briefly discuss two important cases, namely, 4-oxalocrotonate tautomerase (4-OT) and haloalcohol dehalogenase HheC (HheC). The reaction mechanisms of both of these enzymes are quite well established. The reaction of 4-OT involves the creation of an ion pair at the active site, while the reaction of HheC involves the release of a halogen ion. These systems are particularly challenging cases where long-range electrostatics could be expected to influence the energies, and the cluster model might therefore have difficulties providing an accurate description.

The 4-OT enzyme catalyzes the isomerization of unconjugated α-keto acids to their conjugated isomers (Fig. 1a) and is a part of a degradation pathway that converts various aromatic hydrocarbons to citric acid cycle intermediates [12, 13]. The generally accepted mechanism of 4-OT is shown in a simplified version in Fig. 1b. A conserved terminal proline (Pro1) acts as a general base, abstracting a proton from the C-3 position and delivering it back to the C-5 position. Crystallographic and mutational studies have identified three arginine residues as important for the reaction [14–19]. Arg61′ and Arg11′ bind the carboxylate groups of the substrate, and Arg39″ forms a hydrogen bond to the carbonyl oxygen of the substrate, hence stabilizing the negative charge that forms in the transition states and the intermediate state. From the k_{cat} value, the rate-limiting barrier of the 4-OT reaction can be estimated to be approximately 13 kcal/mol. Although the mechanism is quite simple, the reaction of 4-OT represents a rather challenging case to study using the cluster model approach. The charge separation in the intermediate state and the transition states is a feature that might be difficult to handle using a small cluster model of the active site.

In a recent study, two different quantum chemical models of the active site were devised and the potential energy curves for the reaction were computed [20]. The first model (model I, see Fig. 1c) consisted of 77 atoms and contained the substrate, truncated models of Pro1 and the three important arginine residues, and two water molecules. The second model (model II, Fig. 1c) consisted of 177 atoms and contained a number of active-site groups in addition to model I. Larger portions of the side chains of Arg39″, Arg61′, Arg11′, and Pro1 were also kept in the model to grant more flexibility to these groups. With use of these two models, the stationary points along the reaction path were optimized and the potential energy curves were calculated. The surrounding effects were added as single-point calculations using the conductor like polarizable continuum model CPCM [21] using several dielectric constants, $\varepsilon = 2$, 4, 8, 16, and 80. The results are displayed in Fig. 2.

The size of model I is quite small and addition of solvation effects changes the energies significantly (see Fig. 2). As expected, the most pronounced effect is seen for the ion pair intermediate ("Inter" in Fig. 2), for which the energy is lowered by more than 8 kcal/mol upon addition of solvation using $\varepsilon = 80$. Very interestingly, the solvation effects for the larger model II practically vanished (see Fig. 2), i.e., the energy profile is almost identical with and without addition of homogeneous solvation. One can thus consider the cluster model converged. The fact that the model converges already at this size is a quite important and surprising result. Another important difference between the two models is that the energy of the ion-pair intermediate with respect to the reactant Michaelis complex is approximately 7–8 kcal/mol lower for model II compared with model I (including solvation). It can thus be concluded that more groups needed to be added explicitly in the model to provide a proper description of the ion-pair state. Here, it should be mentioned that the energies obtained using the cluster models differ significantly from

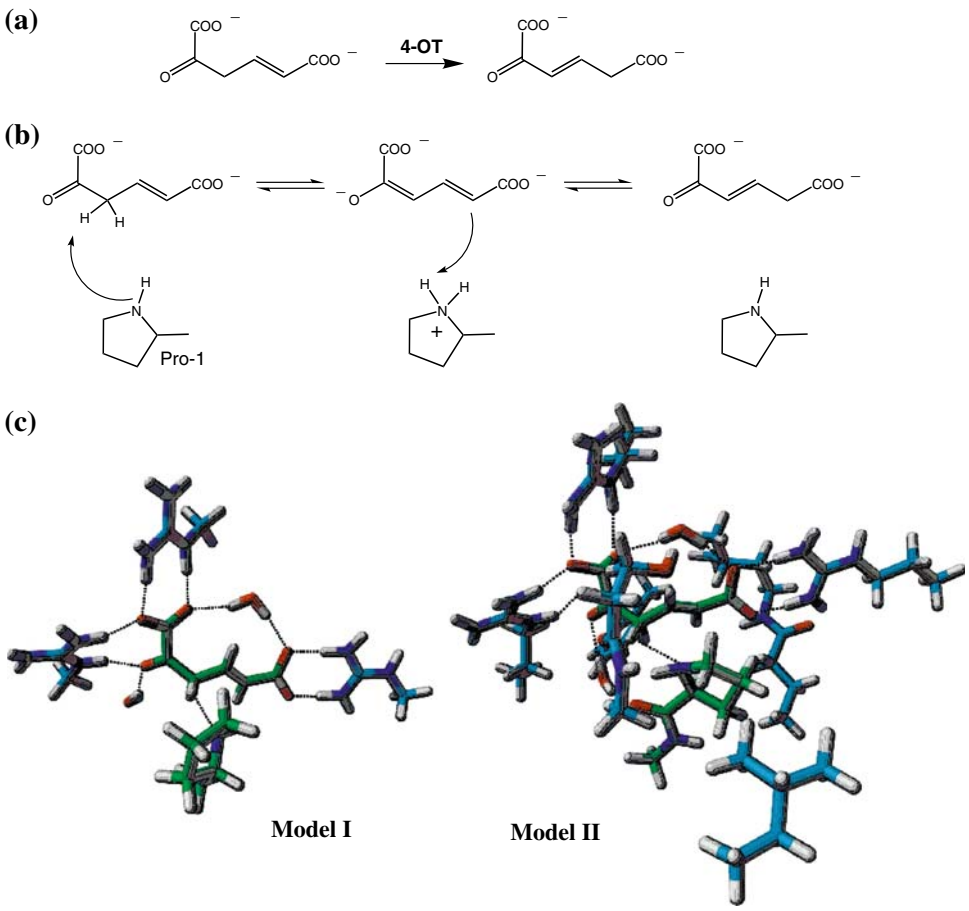

Fig. 1 **a** Reaction catalyzed by 4-oxalocrotonate tautomerase (*4-OT*). **b** Simplified reaction mechanism. **c** Active-site models used

QM/MM results obtained by Cisneros et al. [22–24]. Most notably, the energy of the intermediate is too high in the QM/MM calculations. The results of the cluster model were shown to be more consistent with experimental observations, such as measured relative pK_a values of the substrate and the proline. For detailed discussion, see [20].

The second example of systematic cluster model studies discussed here concerns the dehalogenation reaction of HheC. This enzyme catalyzes the enantioselective conversion of haloalcohols into their corresponding epoxides (Fig. 3a) [25–27]. In addition, it is also able to catalyze the irreversible ring-opening of epoxides with non-halide nucleophiles, such as NO_2^-, CN^-, and N_3^- [28–34].

Also for this enzyme, the reaction mechanism is quite well established (simplified version in Fig. 3b). A tyrosine residue (Tyr145) is proposed to be the catalytic base that abstracts a proton from the halohydrin substrate, upon which the substrate oxyanion displaces the chloride ion through an intramolecular S_N2 reaction. An arginine residue (Arg149) is suggested to activate Tyr145 by abstracting a proton. The free chloride ion is stabilized through interactions in the halide binding site, involving hydrogen bonding to an ordered water molecule and to the backbone amides of Tyr177 and Leu178. It has been shown that the halide release is rate-limiting in HheC. The overall barrier is estimated to be approximately 15 kcal/mol, which means that the barrier for the chemical step should be equal to or less than this amount. Halide ions have large solvation energies, and dehalogenation reactions could thus be difficult to model accurately using quantum chemical models in conjunction with implicit solvent. Cluster models of various sizes were constructed to investigate this reaction [35]. Here we will discuss two of these (models I and II, see Fig. 3c). The small model I consists of 83 atoms and contains the substrate, parts of the side chains of the suggested Arg149-Tyr145-Ser132 catalytic triad, and the backbone carbonyl of Asp80. The halide binding site was modeled by the backbone of Leu178, parts of Phe186, and the crystallographic water molecule. The larger model II, on the other hand, consists of 161 atoms and includes, in addition to model I, a much larger portion of the halide binding site. The main difference is thus in the description of the surroundings of the halide ion. Although the direct hydrogen bonds to the halide are included in both models, the halide atom in model I is quite exposed and the polarizable continuum model cavity can reach all the way to the ion, while in model II the surroundings included will effectively shield the ion. This fact will be reflected in the

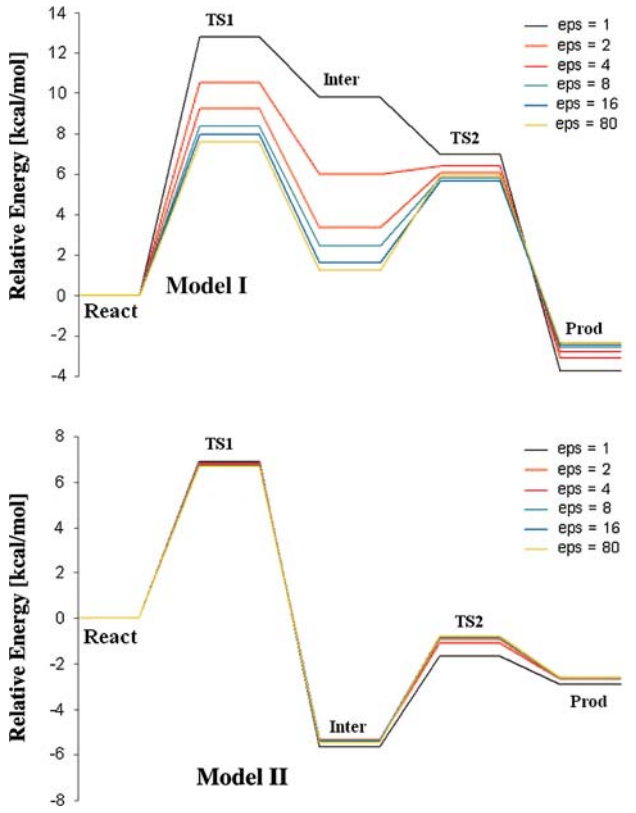

Fig. 2 Calculated potential energy profiles for the 4-OT reaction using the two models of the active site

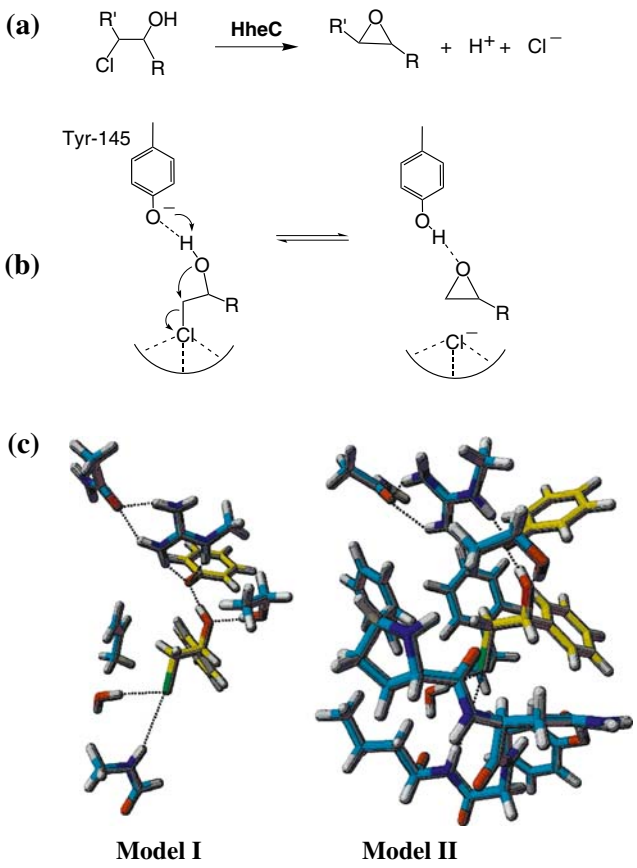

Fig. 3 **a** Reaction catalyzed by haloalcohol dehalogenase HheC (*HheC*). **b** Simplified reaction mechanism. **c** Active-site models used

sensitivity of the energies to the applied solvation. The potential energy graphs obtained using the two models are displayed in Fig. 4.

We note first that both models confirm that the reaction takes place in a single concerted step in which the tyrosinate abstracts a proton from the halohydrin substrate and the substrate oxyanion displaces the chloride ion. The energies obtained with model I are, as expected, quite sensitive to the added homogeneous solvation (see Fig. 4). This model yields a reaction barrier and positive reaction energy for the product state that, without solvation, are strongly overestimated compared with those found from experiments. However, when solvation effects are added using $\varepsilon = 4$, model I reproduces the experimental findings quite nicely. In model II of HheC, as in the case of model II of 4-OT, the energies are practically the same with and without solvation correction, and again the large model must be considered as converged in size.

Comparison of the cluster model with the QM/MM method

To perform calculations using the cluster model with more than 200 atoms is very tedious and hardly practical with present computer resources. Applications on large systems such as enzymes therefore have to rely either on a fast convergence with cluster size using the QM-only method (see earlier) or the accuracy of more approximate methods such as the QM/MM method. When the QM-only and QM/MM methods are compared, it is particularly interesting to investigate cases where the results differ significantly, which is not an uncommon situation in the literature, see for example, [36, 37]. The question is which result should then be trusted most. At present, the conclusion drawn is nearly always that the QM-only result should not be trusted since only a limited model was used, but is this necessarily so? To answer this question, the internal accuracy of the QM/MM method needs to be tested. The internal accuracy of the QM method is assumed to be sufficient since it is used in both methods.

One problem with testing the QM/MM method directly against experiments is that the systems, such as entire enzymes, are so complicated that there can easily be errors from many sources. Errors from the method itself would therefore be mixed with errors in the model and problems of finding proper local minima for a large model, etc. Unfortunately, testing against experiments has still so far

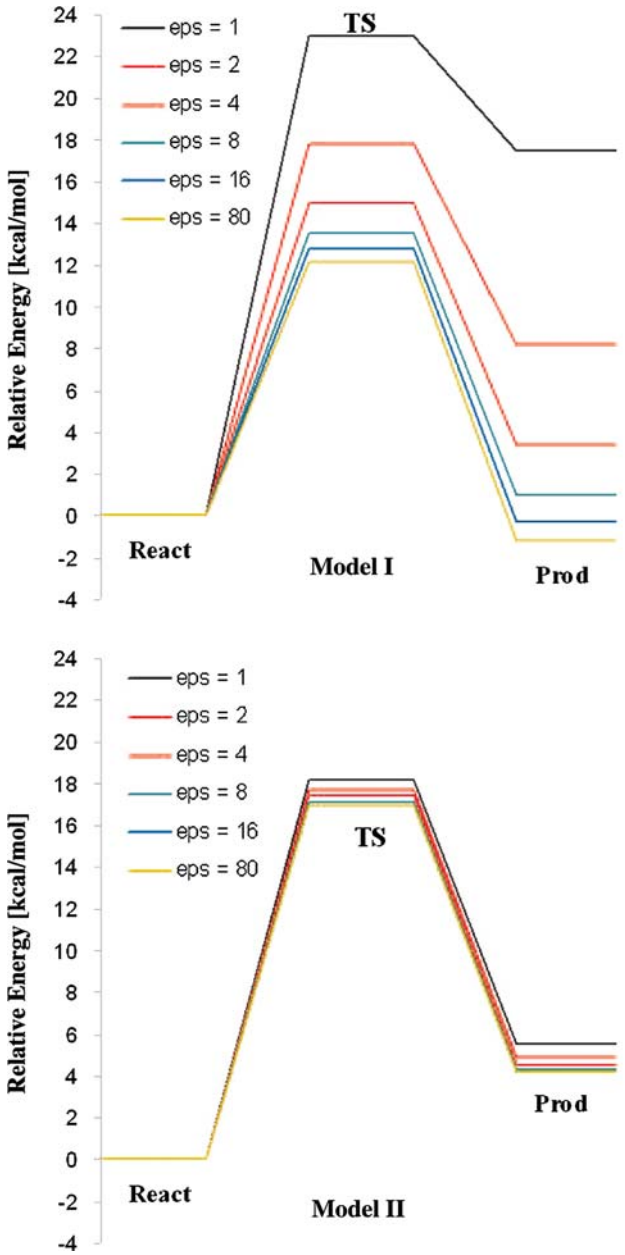

Fig. 4 Calculated potential energy profiles for the HheC reaction using the two models of the active site

been almost the only way that a QM/MM approach has been validated. For a type of convergence test of the QM/MM method different from the ones reported here, see [38, 39]. Owing to the availability of efficient computer codes such as Jaguar [40], it has become possible to test the QM/MM method itself on relatively large systems of 100–200 atoms by a direct comparison with QM-only calculations on the entire system. The same structure could be used for both the QM method and the QM/MM method, or at least the same type of structure, to make sure that the same local minima are compared. Tests of this type were done recently for the ONIOM version [41, 42] of QM/MM in a study of the active site of NiFe hydrogenase [7]. It should be emphasized that the tests described here are only directly applicable for the QM/MM method used. If another QM/MM method were used, other results could well be obtained. Calculations were compared for QM-only and QM/MM models of the active site with 127 and 137 atoms. The QM/MM calculations used 30 QM atoms, which is a common size in earlier applications. This means that the 127-atom model used 97 MM atoms, and the 137-atom model used 107 MM atoms. The 137-atom model is shown in Fig. 5. The 127-atom model only differs by not including the third-shell ligand Asp541. The mechanism goes through a heterolytic cleavage of the H–H bond followed by release of two protons and two electrons. The H–H bond cleavage leads to a bridging hydride and a protonated Cys543. The protons are transferred to the bulk over Cys543.

The energies obtained from the QM-only and QM/MM calculations on the same 127-atom model are shown in Fig. 6. The resulting structures are sketched below the diagrams. The results from the two models are strikingly different in some cases. For example, the ONIOM minimum for Ni_a-SR is as much as 8.2 kcal/mol higher than at the DFT level of theory, and the hydride transfer is 6.1 kcal/mol higher. The differences between the QM and

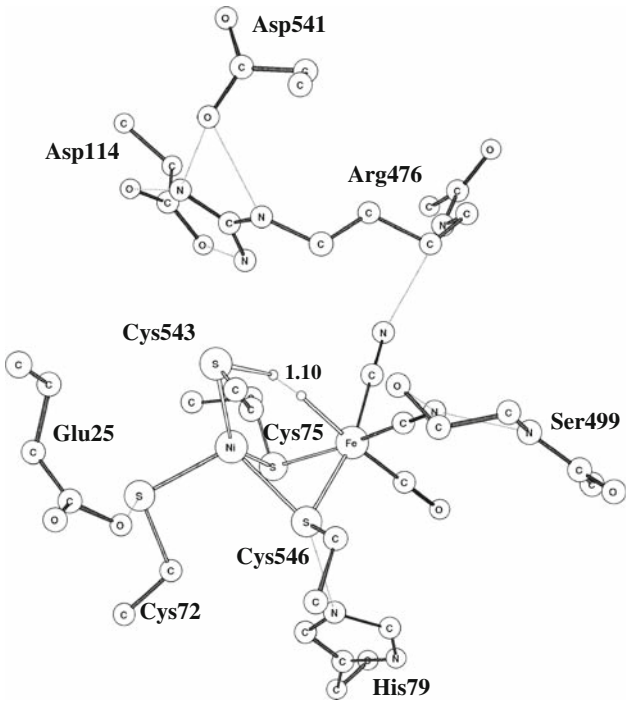

Fig. 5 The 137-atom model of NiFe hydrogenase showing the transition state for heterolytic cleavage of the H–H bond. Hydrogen atoms on the amino acids are omitted for clarity

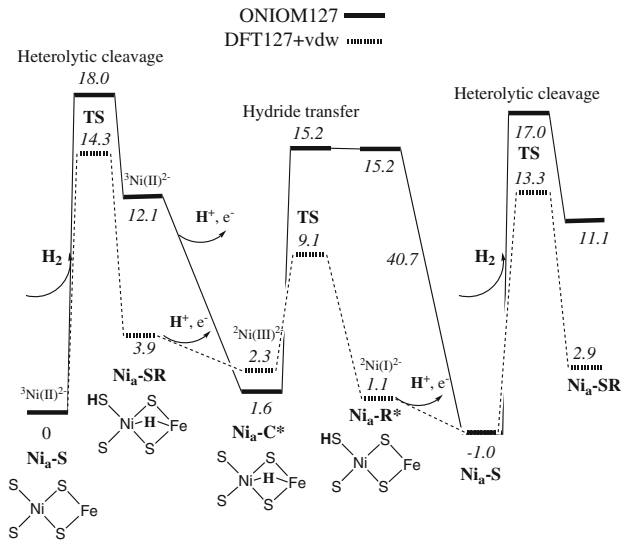

Fig. 6 The density functional theory (*DFT*) and ONIOM results (kcal/mol) for the heterolytic cleavage mechanism using the 127-atom model

QM/MM results must be considered as errors in the QM/MM method from the way the comparison has been made. Of course, the QM DFT results have to be assumed to be correct, but this is assumed also in QM/MM for the QM part. If the same QM/MM method applied on an entire enzyme gave good agreement with experiments, the conclusion would have to be that there are also other errors in the QM/MM calculations which lead to an error cancellation. Such a cancellation of errors has apparently occurred for the 137-atom model; see below. These results are a strong warning against accepting QM/MM results without a careful analysis and validation of the QM/MM model for the particular case of interest. It is possible that a much larger QM part in the QM/MM model might decrease the problems to a sufficient degree. In the present case, a QM part of at least 137 atoms appears to be needed. It is likely that NiFe hydrogenase is particularly difficult owing to the large number of charged groups, and may therefore not be representative for other QM/MM applications, where QM/MM methods have undoubtedly contributed to the current understanding of enzyme mechanisms [2, 43–45].

The sensitivity of the results is further demonstrated by the results for the 137-atom model, for which the QM-only and QM/MM results agree much better (within 3 kcal/mol) [7]. As mentioned above, the good results for the 137-atom model must rely on an error cancellation. Since the only difference between the models is the inclusion of Asp541, this indicates that the description of long-range polarization could be one problem in the QM/MM calculations. Since a standard unpolarizable force field was used in the investigation described here, a polarizable force field might improve the situation.

O–O bond formation in photosystem II, a recent example of the cluster approach

As a final example of the use of the cluster model, a short summary of the results from the most extensive study using this type of model is described. This is a study of oxygen formation at the oxygen-evolving center (OEC) of photosystem II. The investigation has been going on for a decade, but only in recent years have the calculations been based on X-ray structures. However, even at the present stage, the resolution of the X-ray structures is only 3.0–3.5 Å [46, 47]. The result of the X-ray analysis is sketched in Fig. 7. The OEC is formed from a cubane-like cluster with three manganese atoms and one calcium atom connected by μ–oxo bonds, and with a fourth manganese atom outside the cube. Seven amino acids have been indicated as likely ligands of the OEC, but their exact ligation has not been resolved. From the two structures, two different ligation patterns have been suggested: one where several water molecules are also needed to fill up the octahedral coordinations [46], and one where the amino acids fill up most of the ligand positions [47]. One problem with the X-ray structures is that they do not agree with the findings of extended X-ray absorption fine structure (EXAFS) experiments. It has been suggested that this is due to radiation damage [48], but could also come from the low resolution.

One important part of the theoretical model study has been to try to improve the structure. Several models with between 120 and 170 atoms were used in the cluster approach. The backbone positions were held fixed from the X-ray structure, since these positions were considered to be the most accurately determined positions. These positions are furthermore quite similar in the two structures. The ligation pattern from the most recent X-ray structure was adopted [47]. The resulting structure of the S_1 state of the OEC is shown in Fig. 8, where it is placed in the X-ray density. Even though the metal positions are quite different from the ones of the X-ray structures, they fit the density quite well and are therefore at least as accurately positioned as the atoms from the X-ray analysis. Moreover, the

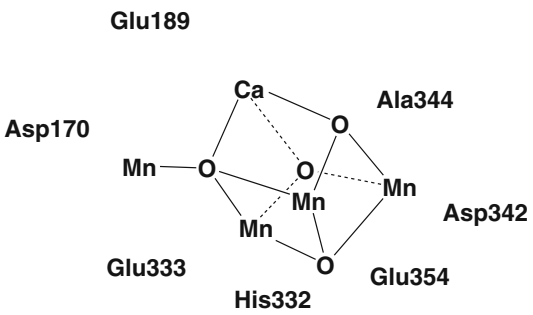

Fig. 7 Simplified picture of the structure of the oxygen-evolving complex, suggested by X-ray crystallography

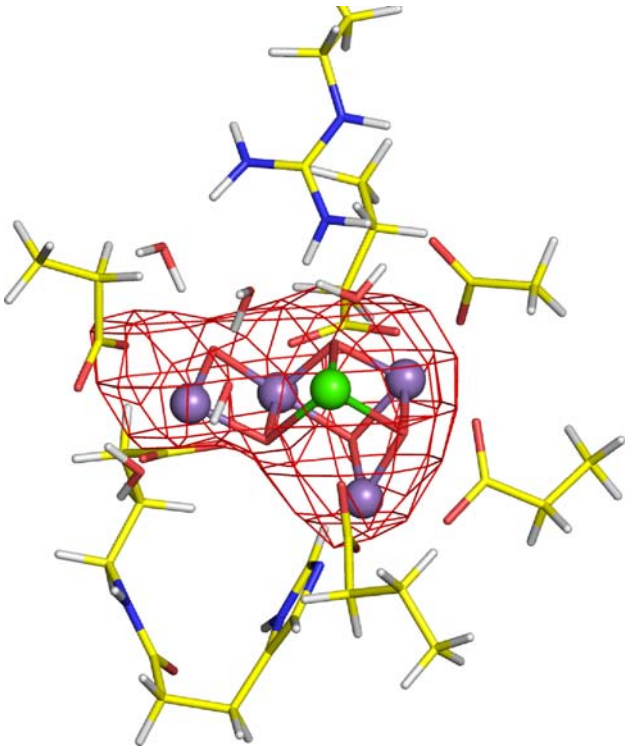

Fig. 8 The DFT-optimized S_1 structure placed into the X-ray density from the London X-ray measurements

metal positions from the calculations, in contrast to the ones from the X-ray structures, are in basic agreement also with those found in at least one EXAFS study [49]: one of the manganese atoms in the cube is only five-coordinate, and there is a short distance between the outer manganese atom and one of the manganese atoms in the cluster.

With the general structure of the OEC described above, all the different steps of water oxidation could then be investigated. The most interesting step is where the O–O bond is formed in the S_4 state. A schematic picture of the transition state is shown in Fig. 9. The most characteristic feature of the O–O bond formation mechanism is that the reactant has an oxygen radical. This radical forms the O–O bond with a μ–oxo ligand, and the barrier is quite low, much lower than for any other mechanism investigated. There is a spin requirement on the transition state for a low barrier with alternating spins between the four atoms involved, the two oxygen atoms and the two manganese atoms to which they are bound [50].

Energy diagrams in good agreement with experimental observations have also been obtained for all the steps of water oxidation. In the early steps, two substrate water molecules become bound to the OEC. The first one binds in a hollow created by the metal atoms. To make space for the binding of the second water molecule, the OEC has to open up in a structural rearrangement in the S_2–S_3 transition, observed experimentally [49] but not rationalized before.

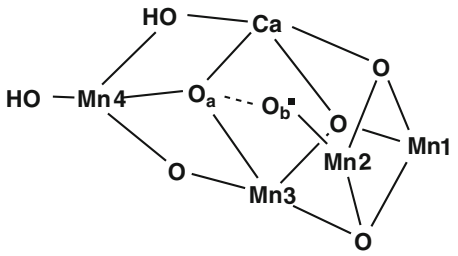

Fig. 9 The transition state for O–O bond formation in the S_4 state

Another characteristic feature observed experimentally is that in the S_1–S_2 transition only an electron is released but no proton. This observation is also rationalized by the model calculations.

Summary

The present standing of the cluster modeling approach for chemical reactions in enzymes has been briefly reviewed. A major recent development in the past few years has been the possibility to use larger and larger QM clusters in the model. This has allowed for more rigorous tests of cluster size convergence. The rather surprising result emerges that the cluster size appears to converge for chemical reactions already in the range 150–200 atoms in many cases. Examples have been given for this in two cases that should be particularly difficult to converge. In one case a relatively large charge separation occurs in the reaction sequence, and in the other a negative halide anion is released. In both cases, long-range electrostatic effects, as probed by dielectric cavity methods, give only very small contributions for the largest model, while they give substantial effects for models smaller than 100 atoms. Similar results have also been obtained in other cases not discussed here. For absolute pK_a values and redox potentials, the dielectric effects are still substantial even for the largest models.

Another advantage of using large QM clusters is that simpler methods such as the QM/MM approach can be tested for more realistic systems. The tests performed on a relatively difficult system with many charged groups show rather large errors for the QM/MM calculations. Further developments of the force fields are therefore suggested to be quite important for obtaining a higher degree of accuracy of QM/MM calculations for this type of system.

Finally, the use of the large QM cluster approach has been described for the case of water oxidation in photosynthesis. The demands on the theoretical study are particularly high in this case since the underlying X-ray structures are still of rather low resolution. Still, it has been demonstrated that results of significant interest and accuracy can be produced by the cluster approach. This

concerns both the mechanism and the structure. Detailed pictures of all the steps of this complicated reaction have been obtained, including the final step of O–O bond formation, in good agreement with available experimental data.

References

1. Siegbahn PEM, Crabtree RH (1997) J Am Chem Soc 119:3103–3113
2. Senn HM, Thiel W (2007) Top Curr Chem 268:173
3. Becke AD (1993) J Chem Phys 98:5648–5652
4. Siegbahn PEM (2006) J Biol Inorg Chem 11:695–701
5. Reiher M, Salomon O, Hess BA (2001) Theor Chem Acc 107:48–55
6. Siegbahn PEM (2007) C R Chim 10:766–774
7. Nilsson Lill SO, Siegbahn PEM (2009) Biochemistry 48:1056–1066
8. Grimme S (2006) J Chem Phys 124:034108
9. Schwabe T, Grimme S (2007) Phys Chem Chem Phys 9:3397–3406
10. Piacenza M, Hyla-Krypsin I, Grimme S (2007) J Comput Chem 28:2275–2285
11. Radon M, Pierloot K (2008) J Phys Chem 112:11824–11832
12. Harayama S, Rekik M, Ngai K-L, Ornston NJ (1989) Bacteriology 171:6251
13. Harayama S, Rekik M (1989) J Biol Chem 264:15328
14. Subramanya HS, Roper DI, Dauter Z, Dodson EJ, Davies GJ, Wilson KS, Wigley DB (1996) Biochemistry 35:792
15. Taylor AB, Czerwinski RM, Johnson WH Jr, Whitman CP, Hackert ML (1998) Biochemistry 37:14692
16. Harris TK, Czerwinski RM, Johnson WH Jr, Legler PM, Abeygunawardana C, Massiah MA, Stivers JT, Whitman CP, Mildvan AS (1999) Biochemistry 38:12343
17. Czerwinski RM, Harris TK, Johnson WH Jr, Legler PM, Stivers JT, Mildvan AS, Whitman CP (1999) Biochemistry 38:12358
18. Metanis N, Brik A, Dawson PE, Keinan E (2004) J Am Chem Soc 126:12726
19. Metanis N, Keinan E, Dawson PE (2005) J Am Chem Soc 127:5862
20. Sevastik R, Himo F (2007) Bioorg Chem 35:444
21. Barone V, Cossi M (1998) J Phys Chem A 102:1995
22. Cisneros GA, Liu H, Zhang Y, Yang W (2003) J Am Chem Soc 125:10384
23. Cisneros GA, Wang M, Silinski P, Fitzgerald MC, Yang W (2004) Biochemistry 43:6885
24. Cisneros GA, Wang M, Silinski P, Fitzgerald MC, Yang WJ (2006) Phys Chem A 110:700
25. Nakamura T, Nagasawa T, Yu F, Watanabe I, Yamada H (1994) Appl Environ Microbiol 60:1297
26. van den Wijngaard AJ, Reuvekamp PTW, Janssen DB (1991) J Bacteriol 173:124
27. van Hylckama Vlieg JET, Tang L, Lutje Spelberg JH, Smilda T, Poelarends GJ, Bosma T, van Merode AE, Fraaije MW, Janssen DB (2001) J Bacteriol 183:5058
28. Janssen DB, Majeric-Elenkov M, Hasnoui G, Hauer B, Lutje Spelberg JH (2006) Biochem Soc Trans 34:291
29. Majeric-Elenkov M, Hauer B, Janssen DB (2006) Adv Synth Catal 348:579
30. Lutje Spelberg JH, van Hylckama Vlieg JET, Tang L, Janssen DB, Kellogg RM (2001) Org Lett 3:41
31. Lutje Spelberg JH, Tang L, van Gelder M, Kellogg RM, Janssen DB (2002) Tetrahedron Asym 13:1083
32. Majeric-Elenkov M, Tang L, Hauer B, Janssen DB (2006) Org Lett 8:4227
33. Hasnaoui G, Lutje Spelberg JH, de Vries E, Tang L, Hauer B, Janssen DB (2005) Tetrahedron Asym 16:1685
34. Nakamura T, Nagasawa T, Yu F, Watanabe I, Yamada H (1991) Biochem Biophys Res Commun 180:124
35. Hopmann KH, Himo FJ (2008) Chem Theor Comput 4:1129
36. Inoue T, Shiota Y, Yoshizawa K (2008) J Am Chem Soc 130:16890–16897
37. Siegbahn PEM (2003) J Biol Inorg Chem 8:567–576
38. Schneboom JC, Lin H, Reuter N, Thiel W, Cohen S, Ogliaro F, Shaik S (2002) J Am Chem Soc 124:8142–8151
39. Altun A, Shaik S, Thiel W (2006) J Comp Chem 27:1324–1337
40. Schrödinger (1991–2003) Jaguar 5.5. Schrödinger, Portland
41. Vreven T, Byun KS, Komaromi I, Dapprich S, Montgomery JA Jr, Morokuma K, Frisch MJ (2006) J Chem Theory Comput 2:815–826
42. Frisch MJ et al (2003) Gaussian 03, revision B.03. Gaussian, Pittsburgh
43. Friesner RA (2005) Adv Protein Chem 72:79–104
44. Riccardi D, Schaefer P, Yang Y, Yu H, Ghosh N, Prat-Resina X, König P, Li G, Xu D, Guo H, Elstner M, Cui Q (2006) J Phys Chem B 110:6458–6469
45. Senthilkumar K, Mujika JI, Ranaghan KE, Manby FR, Mulholland AJ, Harvey JN (2008) J R Soc Interface 5:S207–S216
46. Ferreira KN, Iverson TM, Maghlaoui K, Barber J, Iwata S (2004) Science 303:1831–1838
47. Loll B, Kern J, Saenger W, Zouni A, Biesiadka J (2005) Nature 438:1040–1044
48. Yano J, Kern J, Irrgang K-D, Latimer MJ, Bergmann U, Glatzel P, Pushkar Y, Biesiadka J, Loll B, Sauer K, Messinger J, Zouni A, Yachandra VK (2005) Proc Natl Acad Sci USA 102:12047–12052
49. Dau H, Grundmeier A, Loja P, Haumann M (2008) Philos Trans R Soc Lond B 363:1237–1244
50. Siegbahn PEM (2006) Chem Eur J 12:9217–9227